ORIGINAL PAPER

Yu-Shuan Shiau · Tze-Bin Lin · Horng-Huey Liou
Po-Tsarng Huang · Kuo-Long Lou · Yuh-Yuan Shiau

Molecular simulation reveals structural determinants of the hanatoxin binding in Kv2.1 channels

Abstract The carboxyl terminus of the S3 segment (S3$_C$) in voltage-gated potassium channels was suggested to be the binding site of gating modifier toxins like hanatoxin. It has also been proposed to have a helical secondary structural arrangement. The currently available structures in high resolution for such channel molecules are restricted to regions illustrating the pore function. Therefore no further direct experimental data to elucidate the detailed mechanism for such toxin binding can be derived. In order to examine the putative three-dimensional structure of S3$_C$ and to analyze the residues required for hanatoxin binding, molecular simulation and docking were performed, based on the solution structure of hanatoxin and the structural information from mutational scanning data for the S3$_C$ fragment in Kv2.1. Our results indicate that hydrophobic and electrostatic interactions are both utilized to stabilize the toxin binding. Precise docking residues and the appropriate orientation for binding regarding amphipathic environments are also described. Compared with the functional data proposed by previous studies, the helical structural arrangement for the C-terminus of the S3 segment in voltage-gated potassium channels can therefore be further emphasized and analyzed. The possible location/orientation for toxin binding with respect to membrane distribution around the S3$_C$ segment is also discussed in this paper.

Y.-S. Shiau
Department of Entomology, National Taiwan University,
Taipei, Taiwan

T.-B. Lin
Department of Physiology, Chung-Shan Medical University,
Taichung, Taiwan

H.-H. Liou
Department of Pharmacology, Medical College,
National Taiwan University, Taipei, Taiwan

Y.-S. Shiau · P.-T. Huang · K.-L. Lou (✉) · Y.-Y. Shiau
Graduate Institute of Oral Biology, Medical College,
National Taiwan University, Chang-Teh Str. 1,
Taipei 10042, Taiwan
e-mail: kllou@ntumc.org
Tel.: +886-2-23123456 ext. 6616, Fax: +886-2-23820785

Introduction

The voltage-gated K$^+$ channels comprise a large family of tetrameric membrane proteins that open and close in response to changes in membrane voltage. Six putative transmembrane segments termed S1 through S6 are included in each subunit of the tetramer. Among them, S5 through S6 assemble the central pore domain forming the K$^+$-selective ion conduction pathway. [1, 2, 3, 4, 5, 6, 7, 8, 9, 10] The crystal structure of a relatively simple prokaryotic K$^+$ channel, KcsA, with two transmembrane segments in each subunit that are homologous to S5–S6 in voltage-gated K$^+$ channels suggests that S5 and S6 are undoubtedly membrane spanning α-helices with the S5–S6 linker containing the most conserved region of all K$^+$ channels. This region forms a short pore helix and the selectivity filter. [11, 12] The first four transmembrane segments (S1–S4) of voltage-gated K$^+$ channels do not contribute to the simple pore as in KcsA and in the inward rectifier K$^+$ channels, and appear to have their unique voltage-sensing capabilities. [10] However, the high-resolution structure of S1–S4 and a functional interpretation derived from it to illustrate the voltage-sensing mechanism are still not clear.

S4 is an unusual transmembrane segment that contains a large number of basic residues, which has been suggested by many studies be strongly involved in sensing changes in the membrane voltage. [13, 14, 15, 16, 17, 18, 19, 20, 21, 22, 23] In addition, a growing body of evidence suggests that S2 and S3 may also participate in voltage-sensing, especially S3. [19, 24, 25, 26, 27, 28, 29, 30, 31, 32, 33, 34, 35] The C-terminal part of the S3 segment (S3$_C$) is of particular interest because it has been identified as an important region for interaction with various gating modifier toxins. [31, 32, 34, 36, 37, 38] Among them, hanatoxin (HaTx1), a 35-amino acid protein isolated from tarantula venom, [39] shows an in-

hibition on the Kv2.1 (*drk1*) channel, which belongs to the *shab* K⁺ channel family, by shifting activation to more depolarized voltages. [40]

Recently, the solution structure of HaTx1 [33] has been determined and the hydrophobic patch, whose residues may interact with Kv2.1 upon binding, was described. The mechanism for inhibition by this toxin is quite unique and distinct from other previously described K⁺ channel inhibitors. HaTx1 binds to Kv2.1 in each of the four voltage-sensing domains, not by blocking the pore, to achieve the inhibition. [37] As previously described, $S3_C$ has been proposed as the exact binding site. [31, 32, 35, 37, 38] In the tryptophan-, alanine-, and lysine-scanning mutagenesis studies, a short non-helical stretch or kink of a conserved proline residue in the S3 transmembrane segment was observed and its possible role in structural arrangement was discussed. [31, 32, 35, 41, 42, 43, 44, 45, 46] Meanwhile, the existence of two helical fragments ($S3_N$ and $S3_C$) for this segment, therefore, has been proposed after the helical periodicity was analyzed. [31, 32, 35]

However, the structural information illustrating the precise residues required for HaTx1–Kv2.1 binding and the thus derived molecular mechanisms are still absent because of the lack of a complete structure of voltage-gated potassium channels at high resolution. In the present study, we have systematically docked the two molecules by presenting HaTx1 with its solution structure and Kv2.1 by modeling the C-terminus of S3 with restraints based on the possible structural arrangement of the α-helix deduced from previous mutational scanning data. The molecular determinants needed to stabilize the hanatoxin binding in Kv2.1, which then further results in the inhibition of channel gating, can therefore be described through such a docking simulation. Organization of the transmembrane helices implying their spatial freedom may lead to other interesting points.

Materials and methods

Model building

Kv2.1 S3$_C$ fragment

The Kv2.1 $S3_C$ molecule (Val-271 to Val-282, amino acid sequence: VTIFLTESNKSV) was constructed via modification from a fragment dictionary with geometry optimized using the consistent valence force field (CVFF) with the Biopolymer module of the Insight II software package (Accelrys Inc., U.S.A.). Atomic charges were computed using the semiempirical MO-PAC/AM1 method. The residues based on the prediction of an α-helix were individually regularized by energy minimization to give reasonable geometries.

HaTx1 structure

The coordinates for HaTx1 were obtained from the Brookhaven Protein Databank in a pdb file (PDB ID number 1D1H). The surface charge distribution of the toxin molecule was displayed by performing the Connolly surface operation.

Docking simulation

Determination of starting orientations

In principle, three criteria were used to determine the starting positions: (i) stereochemistry, (ii) side-chain charge distribution, and (iii) previous structural information. Inappropriate possibilities have been immediately excluded if definitely unreasonable combinations of alignment for docking were observed. Uncertain orientations were reserved and submitted for docking calculation to allow the computational results to perform the screening.

Calculation for the energies

Upon docking, the total energies of electrostatic interactions and van der Waals contacts between the complexes of HaTx1 and $S3_C$-binding model were compared. All docked complexes were subjected to 20 runs. Each run was composed of 500 cycles of simulated annealing and 1,000,000 steps of accepted/rejected configurations.

The values of all other default parameters were used. The alignment between docked and undocked molecules was performed by manually fitting the atomic coordinates of groups of residues that may be involved in the conserved interaction. Briefly, three-dimensional (3D) surfaces of the binding site enclose the most active members (after appropriate alignment) of the starting set of molecules. Note that errors in alignment can lead to incorrect, poorly predictive receptor surface models. This problem was overcome by using information obtained from previously related functional data. The surface was generated from a "shape field", in which the atomic coordinates of the contributing models were used to compute field values on each point of a 3D grid using a van der Waals function. A solvation energy correction term and the electrostatic charge complementarity method were used for energy evaluation. The solvation energy correction term is a penalty function that attempts to account for the loss of solvation energy when polar atoms are forced into hydrophobic regions of the receptor surface. All the calculations and structure manipulations described above were performed with the Discover and Docking/Insight II (2000) molecular simulation and modeling program (Molecular Simulation, San Diego, Calif., U.S.A.; 950 release) on a Silicon Graphics Octane/SSE workstation.
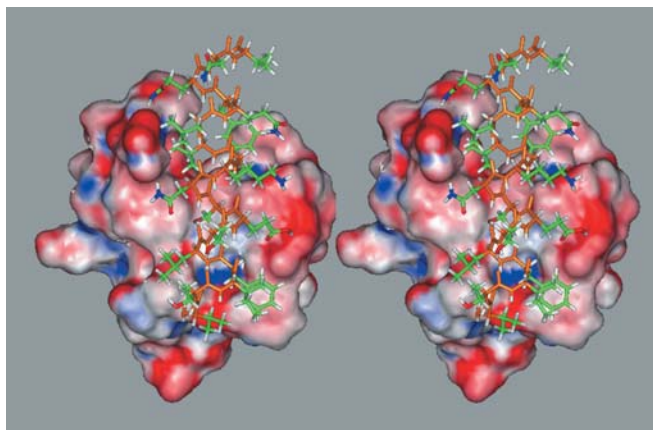
Fig. 1 Stereo diagram of the docking complex. The electrostatic potential surfaces are shown for HaTx1, in which *red* corresponds to an electrostatic potential of $<-5\ k_BT/e$, *white* $0\ k_BT/e$ and *blue* of $>+5\ k_BT/e$. The main chain of the Kv2.1 S3$_C$ molecule is drawn with thick sticks in *orange*, while the side chains with sticks in color according to the types of atoms. The detailed binding area including residues required for binding is enlarged in Fig. 2

Fig. 2a,b Stereo diagrams for close view of the HaTx1–Kv2.1 binding site. The main chains in both molecules are shown with ribbons in *orange* (Kv2.1) and in *magenta* (HaTx1), respectively. Residues required to form interactions between the two molecules are properly labeled with distances indicated. **a** The hydrophobic/aromatic contacts. **b** Electrostatic interactions

Results and discussions

The hydrophobic patch on the HaTx1 surface [33] was very useful in providing directions for choices. Most of the docking combinations were commenced based on the search for appropriate residues of the S3$_C$ helix to interact with the hydrophobic patch. The leading concern at this stage was the residue type that satisfied both with regard to stereochemistry and hydrophobic/aromatic interactions, for which we took the residues suggested by Swartz and co-workers [31, 32, 35] into consideration and at the same time compared with the structural effects they might bring in three dimensions. After such observation, the residues required for hydrophobic interactions were defined for that orientation, and then the residues surrounding the hydrophobic patch were analyzed. The electrostatic interaction was therefore the major premise for this step.

Several possible conformations were chosen and submitted for docking calculation. In Fig. 1, the docking orientation with the best energy results after the simulation is shown, with respect to both the electrostatic energy (–35.71 kcal mol⁻¹) and the van der Waals contacts (268.85 kcal mol⁻¹).

With such an orientation, hydrophobic contacts should occur between Kv2.1 residue side chains of Val-271, Phe-274, Leu-275, Val-282 and the residue side chains of Leu-5, Phe-6, Tyr-27, Ala-29, Trp-30 from the hydrophobic patch in HaTx1 (Fig. 2a). In addition, there are several charged or polar residues surrounding this area to form electrostatic interactions with residues from HaTx1, which stabilize the binding between HaTx1 and Kv2.1 in a more efficient way (Fig. 2b). For example, salt-bridges were found between side-chain atoms of Arg-24 from HaTx1 and Glu-277 from Kv2.1, whereas

hydrogen-bonding networks were observed between Tyr-27 (HaTx1), Asp-25 (HaTx1) and Ser-281 (Kv2.1), Glu-277 (Kv2.1). In addition, intramolecular interactions appeared in HaTx1 after the docking simulation: a salt-bridge between Arg-24 and Asp-25 and H-bonds for Tyr-27 and Asp-25. These are crucial interactions on the right-hand side of the S3$_C$ helix (as seen in Fig. 2b). On the left-hand side, another close interaction was found between Ser-35 from HaTx1 and Asn-279 from Kv2.1. Such an observation explains and verifies the reasonable requirement of those charged residues flanking the hydrophobic patch in hanatoxin for the toxin–channel binding function. [33]

We have systematically docked the two molecules by presenting HaTx1 with its solution structure [33] and Kv2.1 by modeling the C-terminus of S3 with restraints based on the possible structural arrangement of the α-helix deduced from previous mutational scanning data. [35] From our results, the precise residues required for hanatoxin binding onto voltage-gated potassium channel Kv2.1 are described (Fig. 2). With respect to this point, we found that both hydrophobic and electrostatic interactions are required to stabilize the toxin-channel binding. This confirms and expands the idea proposed by Takahashi and co-workers. [33]

The location for HaTx1 binding, regarding the vicinity of S3$_C$ in Kv2.1, must be further discussed here. Figure 3 illustrates our speculations. Those S3$_C$ residues that interact with the hydrophobic patch of HaTx1 would not be tolerated in the aqueous phase of extracellular space outside the channels. Deep integration into the membrane will also be too hard for the toxin to penetrate and reach the site for binding. Therefore, these residues

Fig. 3a,b Cartoon illustrating the approximate location and orientation for HaTx1 binding onto Kv2.1. **a** The six transmembrane segments S1 to S6 are arranged according to the model proposed by Cha and co-workers. [29] HaTx1 binds to the approximate location as discussed in the text. External crevice and putative direction for potassium ion flux are also indicated. **b** Local enlarged top view of **a**. The helical wheel for Kv2.1 $S3_C$ is presented to allow the comprehension for relative spatial organization between $S3_C$, HaTx1, external crevice, and, speculatively, S4 [49]

must be located at the boundary of membrane, closely below the hydrophilic heads of the membrane phospholipids (similar to the role the aromatic rings play in membrane proteins). Considering that, the $S3_C$ helix is in an orientation keeping a tilt angle compared to the axis perpendicular to the membrane. In this case, $S3_C$ can be regarded approximately as two parts (Fig. 3). One part is the hydrophobic/aromatic area we have just discussed. HaTx1 should bind to this area from the direction more to the side surface of the $S3_C$ helix, instead of approaching it from the top, which would mean binding towards the face exposed to the extracellular solvents. The other part of the $S3_C$ helix, according to our observations, includes the residues facing the external crevice [29] that allows S4 to move while gating. [17, 21, 22, 47, 48, 49]

It is not difficult to find supporting information by checking the $S3_C$ residues, with respect to both residue types and the positions in the helical wheel (Fig. 3b), which decides the environments that the residue side

chains have to face or to be exposed to. Besides, it seems quite impossible to further investigate the spatial relation between $S3_C$ and the N-terminus of S4 at this moment, without sufficient restraints that we can use to perform similar molecular simulations.

Conclusion

Our structural analysis with docking simulation has for the first time provided objective and fairly direct evidence for describing how hanatoxin and the voltage-gated potassium channel Kv2.1 interact upon binding. Further implication to explain the inhibition of gating induced by such toxin binding [49] can rely on the structural and functional characterizations based on our results. Nevertheless, the structural information described in this paper should be sufficient to provide directions for more electrophysiological examination in details.

References

1. MacKinnon R, Miller C (1989) Science 245:1382–1385
2. MacKinnon R, Yellen G (1990) Science 250:276–279
3. Hartmann HA, Kirsch GE, Drewe JA, Taglialatela M, Joho RH, Brown AM (1991) Science 251:942–944
4. MacKinnon R (1991) Nature 350:232–235
5. Yellen G, Jurman ME, Abramson T, MacKinnon R (1991) Science 251:939–942
6. Yool AJ, Schwarz TL (1991) Nature 349:700–704
7. Liman ER, Tytgat J, Hess P (1992) Neuron 9:861–871
8. Heginbotham L, Lu Z, Abramson T, MacKinnon R (1994) Biophys J 66:1061–1067
9. Ranganathan R, Lewis JH, MacKinnon R (1996) Neuron 16:131–139
10. Armstrong CM, Hille B (1998) Neuron 20:371–380
11. Schrempf H, Schmidt O, Kummerlen R, Hinnah S, Müller D, Betzler M, Steinkamp T, Wagner R (1995) EMBO J 14:5170–5178
12. Doyle DA, Morais-Cabral J, Pfuetzner RA, Kuo A, Morais Gulbis J, Cohen SL, Chait BT, MacKinnon R (1998) Science 280:69–77
13. Liman ER, Hess P, Weaver F, Koren G (1991) Nature 353:752–756
14. Papazian DM, Timpe LC, Jan YN, Jan LY (1991) Nature 349:305–310
15. Perozo E, Santacruz-Toloza L, Stefani E, Bezanilla F, Papazian DM (1994) Biophys J 66:345–354
16. Aggarwal SK, MacKinnon R (1996) Neuron 16:1169–1177
17. Larsson HP, Baker OS, Dhillon DS, Isacoff EY (1996) Neuron 16:387–397
18. Mannuzzu LM, Moronne MM, Isakoff EY (1996) Science 271:213–216
19. Seoh SA, Sigg D, Papazian DM, Bezanilla F (1996) Neuron 16:1159–1167
20. Yang N, George Jr AL, Horn R (1996) Neuron 16:113–122
21. Smith-Maxwell CJ, Ledwell JL, Aldrich RW (1998) J Gen Physiol 111:399–420

22. Smith-Maxwell CJ, Ledwell JL, Aldrich RW (1998) J Gen Physiol 111:421–439
23. Ledwell JL, Aldrich RW (1999) J Gen Physiol 113:389–414
24. Frech GC, van Dongen AM, Schuster G, Brown AM, Joho RH (1989) Nature 340:642–645
25. Papazian DM, Shao XM, Seoh SA, Mock AF, Huang Y, Wainstock DH (1995) Neuron 14:1293–1301
26. Planells-Cases R, Ferrer-Montiel AV, Patten CD, Montal M (1995) Proc Natl Acad Sci USA 92:9422–9426
27. Cha A, Bezanilla F (1997) Neuron 19:1127–1140
28. Tiwari-Woodruff SK, Schulteis CT, Mock AF, Papazian DM (1997) Biophys J 72:1489–1500
29. Cha A, Snyder GE, Selvin PR, Bezanilla F (1999) Nature 402:809–813
30. Monks SA, Needleman DJ, Miller C (1999) J Gen Physiol 113:415–423
31. Li-Smerin Y, Hackos DH, Swartz KJ (2000) J Gen Physiol 115:33–50
32. Li-Smerin Y, Swartz KJ (2000) J Gen Physiol 115:673–684
33. Takahashi H, Kim JI, Min HJ, Sato K, Swartz KJ, Shimada I (2000) J Mol Biol 297:771–780
34. Winterfield JR, Swartz KJ (2000) J Gen Physiol 116:637–644
35. Li-Smerin Y, Swartz KJ (2001) J Gen Physiol 117:205–218
36. Rogers JC, Qu Y, Tanada TN, Scheuer T, Catterall WA (1996) J Biol Chem 271:15950–15962
37. Swartz KJ, Mackinnon R (1997) Neuron 18:675–682
38. Li-Smerin Y, Swartz KJ (1998) Proc Natl Acad Sci USA 95:8585–8589
39. Swartz KJ, Mackinnon R (1995) Neuron 15:941–949
40. Swartz KJ, Mackinnon R (1997) Neuron 18:665–673
41. O'Neil KT, DeGrado WF (1990) Science 250:646–651
42. MacArthur MW, Thornton JM (1991) J Mol Biol 218:397–412
43. Blaber M, Zhang XJ, Matthews BW (1993) Science 260: 1637–1640
44. Mathur R, Zheng J, Yan Y, Sigworth FJ (1997) J Gen Physiol 109:191–199
45. Monne M, Hermansson M, von Heijne G (1999) J Mol Biol 288:141–145
46. Hong KH, Miller C (2000) J Gen Physiol 115:51–58
47. Bezanilla F, Perozo E, Papazian DM, Stefani E (1996) Science 254:679–683
48. Yusaf SP, Wray D, Sivaprasadarao A (1996) Pflüg Arch 433:91–97
49. Huang PT, Liou HH, Lin TB, Chen TY, Spatz HC, Tseng LJ, Shiau YY, Lou KL (2002) Recept Channels 8:79–85